Supporting Information

Enhanced Collision Induced Unfolding and Electron Capture Dissociation of Native-like Protein Ions

Varun V. Gadkari[†], Carolina Rojas Ramírez [†], Daniel D. Vallejo[†], Ruwan T. Kurulugama[‡], John C. Fjeldsted[‡], and Brandon T. Ruotolo[†*]

[†]Department of Chemistry, University of Michigan. 930 North University Avenue, Ann Arbor, Michigan, United States
[‡]Agilent Technologies, 5301 Stevens Creek Blvd, Santa Clara, California 98051

[*]Corresponding Author: **Phone:** 1-734-615-0198. **Fax:** 1-734-615-3718. **E-mail:** bruotolo@umich.edu.

Table of Contents

Figure S1

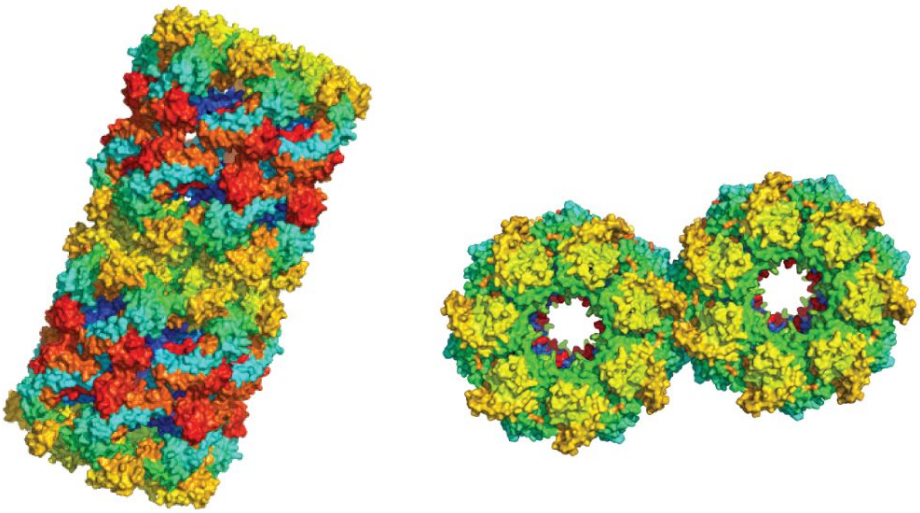

Figure S1: IMPACT CCS measurements of 28mer models

PDB structure 5W0S, of 14-mer GroEL was used to make two types of 28-mer complexes that we envision, referred to as "vertical stack" and "side stack." Using IMPACT we computed the CCS of the structures. The projection approximation of each complex is reported.

Figure S2

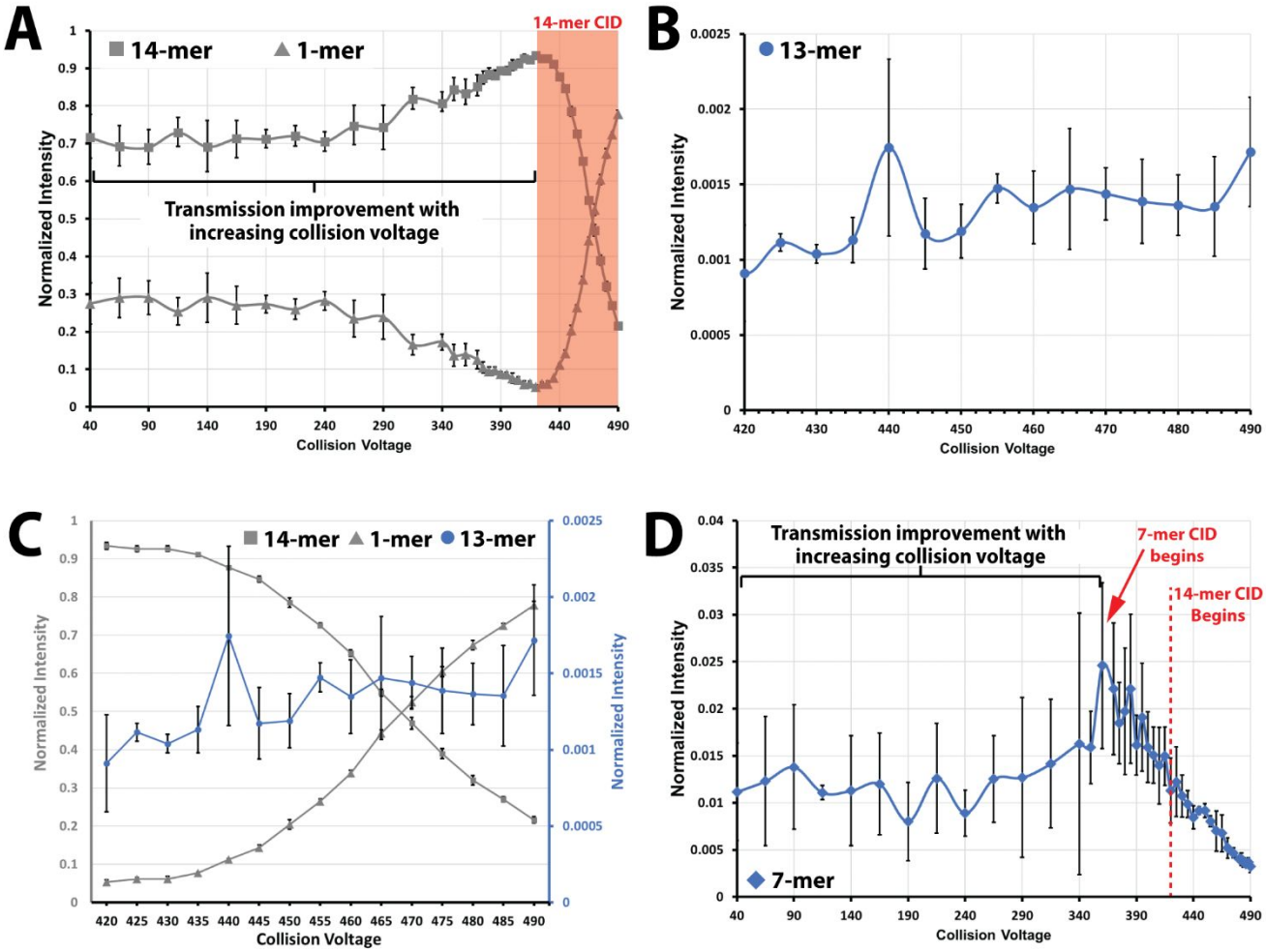

Figure S2: Collision Induced Dissociation of GroEL

(A) Collision induced dissociation (CID) of GroEL 14-mer complex (grey squares) results in the ejection of monomers ("1-mer" grey triangles) and formation of a 13-mer stripped complex (blue circles). 14-mer signal steadily increases from 40 V in-source collision voltage, until 420 V. This is attributed to the improvement in transmission of the larger ions due to higher source voltages. Starting at 420 V the 14-mer complex begins to dissociate by CID, ejecting GroEL monomers. The decrease in 14-mer signal, with the concomitant increase in monomer signal is observed from 420 V to 490 V (end of experiment); this region of the normalized intensity plot is shaded in red. **(B)** The stripped complex in native protein complex CID is typically a low intensity species due to inefficient transmission as a result of ion focusing issues. In our experiments, we see a slight increase in 13-mer normalized intensity between 420 and 490 volts. The mass spectrum for this complex is show in **Figure 2E**. **(C)** The 14-mer, 13-mer, and monomer normalized intensities are plotted together to corelate the increase of 13-mer and monomer normalized intensity, with the decrease of 14-mer normalized intensity. The 13-mer normalized intensity is represented by the blue secondary y-axis. The 14-mer and monomer signal is represented by the grey primary y-axis. **(D)** The 7-mer complex (blue diamonds) was also observed in this experiment. It was present in solution before gas phase activation, as shown in **Figure 2A**. Similar to the 14-mer signal intensity, the signal for the 7-mer slightly increases initially as a result of improved large ion transmission at higher source voltages. Starting at 360 V, the 7-mer begins fragmenting as a result of CID, as indicated by the steep decline in 7-mer signal. The CID products are not detected due to the low starting intensity of the parent ion (norm. int. of 0.025). A red dotted line at 420 V denotes the start of parallel 14-mer CID. The abundance of the 7-mer is unaffected, suggesting that there is no dissociation of 14-mer complex into 7-mer.

Figure S3

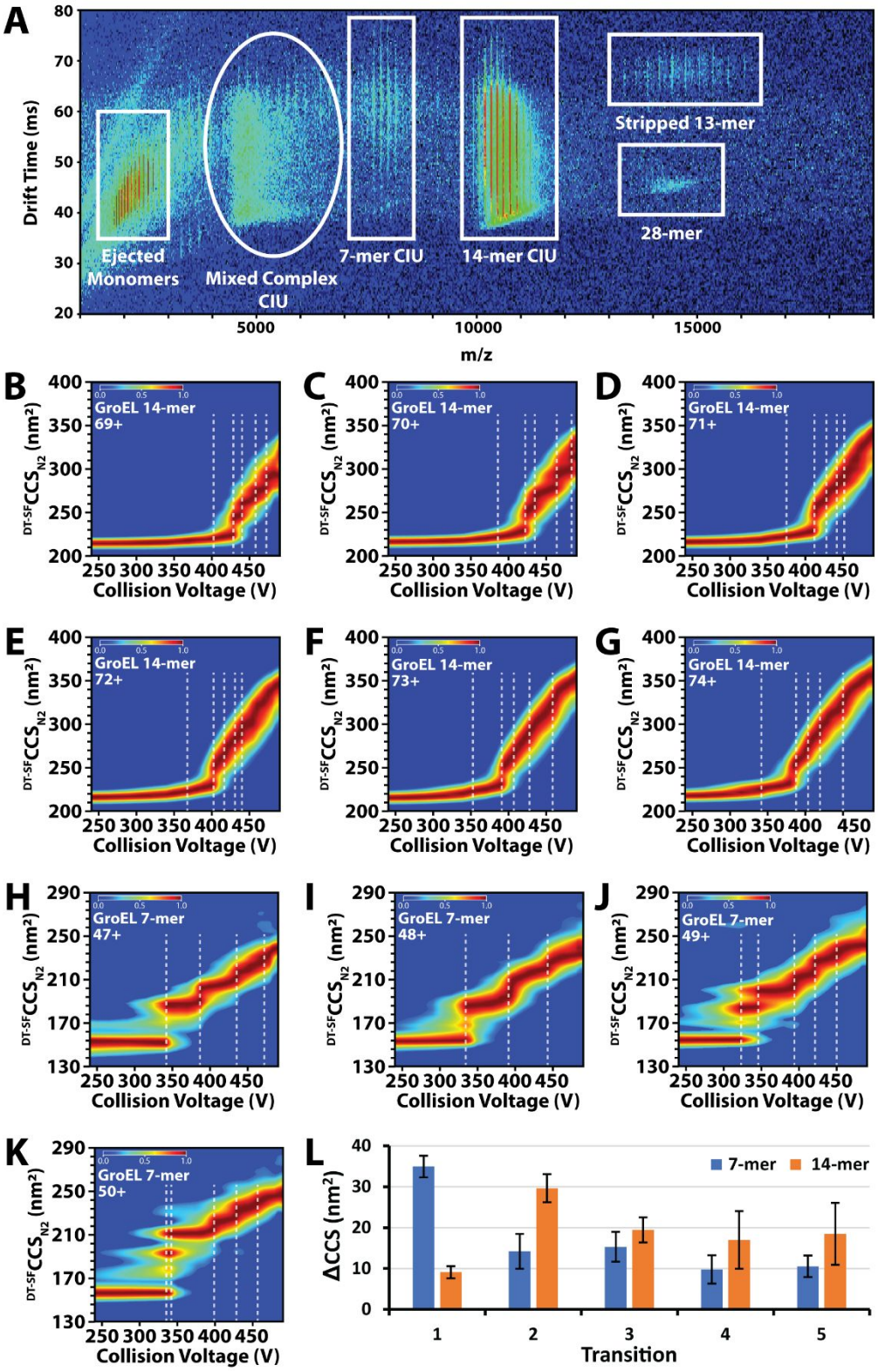

Figure S3: CIU of GroEL complexes

(A) IM-MS spectrum integrated across entire CIU experiment, increasing in-source activation from 50 V to 490 V. The various species observed are labeled. **(B-G)** CIU of 69+ to 74+ charge states of GroEL 14-mer. **(H-K)** CIU of 47+ to 50+ charge states of GroEL 7-mer. **(L)** Comparison of the ΔCCS between the first 5 CIU transitions GroEL 7-mer (blue) and GroEL 14-mer (orange). The dotted lines on the CIU fingerprints indicate the transitions, T1 to T5 left to right, Some fingerprints had less than 5 transitions. At least 2 transition ΔCCS values were observed for each transition compared in **(L)** and the bar plotted represents the average of these values. The error bar represents standard deviation.

Figure S4

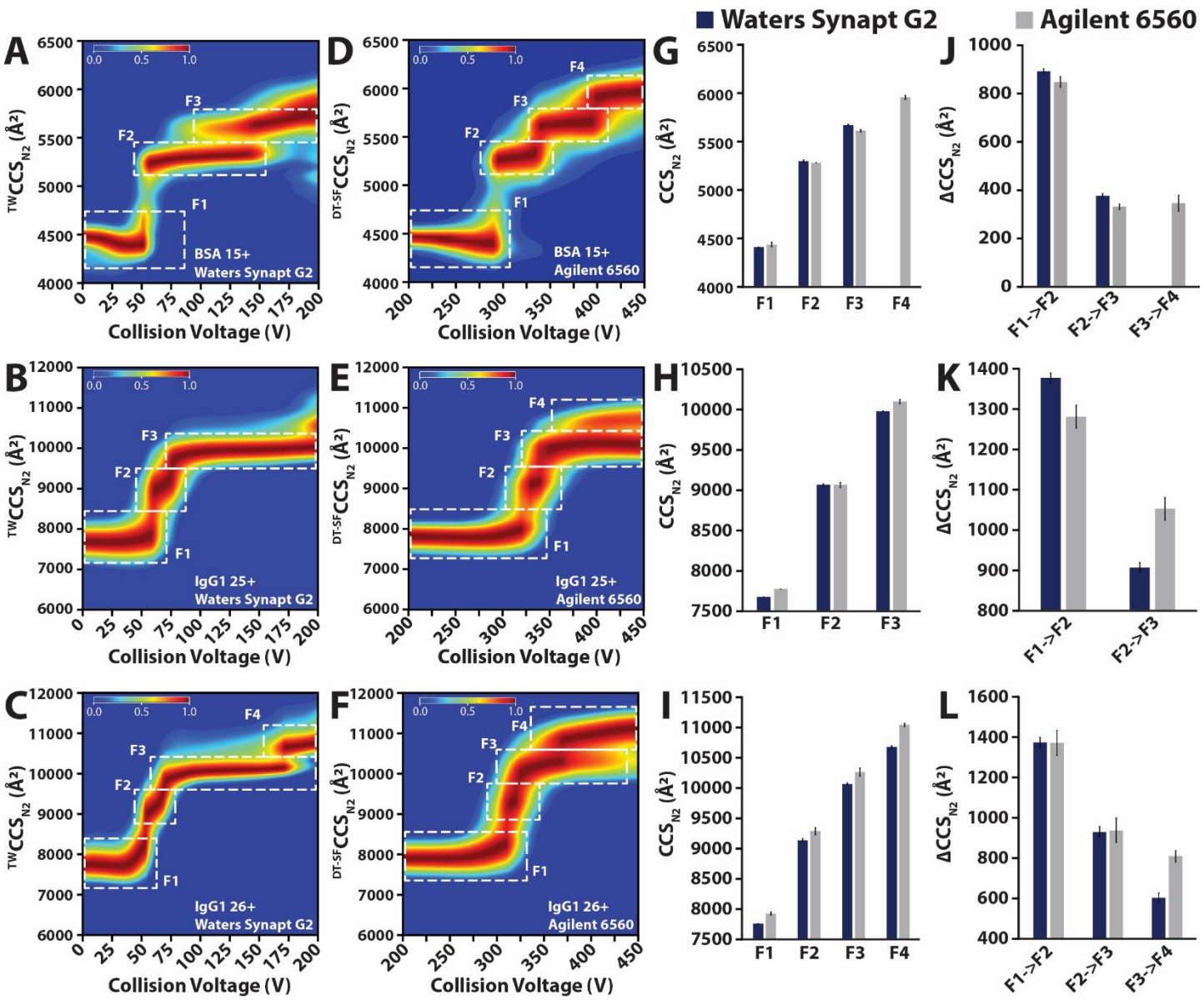

Figure S4: Comparison of CIU on Agilent 6560 vs. Waters Synapt G2

As reported in the main text, when comparing CIU fingerprints of the same protein between the Waters Synapt G2 and Agilent 6560, the CCS_{N2} of the CIU features do not align exactly. However, at most features between two instruments are within 2.4% of each other, additionally the ΔCCS comparisons show that the changes in CCS between features are similar between instruments. **(A-C)** CIU of BSA 15+, IgG1 25+, and IgG1 26+ respectively on the Waters Synapt G2. **(D-F)** CIU of BSA 15+, IgG1 25+, and IgG1 26+ respectively on the Agilent 6560. **(G-I)** Comparison of BSA 15+, IgG1 25+, and IgG1 26+ feature CCS_{N2} respectively between the Waters Synapt G2 (blue bars) and Agilent 6560 (grey bars). **(J-L)** Comparison of BSA 15+, IgG1 25+, and IgG1 26+ feature ΔCCS_{N2} respectively between the Waters Synapt G2 (blue bars) and Agilent 6560 (grey bars). CIU fingerprints are an average of at least 3 independent experiments. The CCS and ΔCCS reported in the bar charts are averages from feature fitting each of the replicates for each experiment. The error bar represents the standard deviation between replicates.

Figure S5

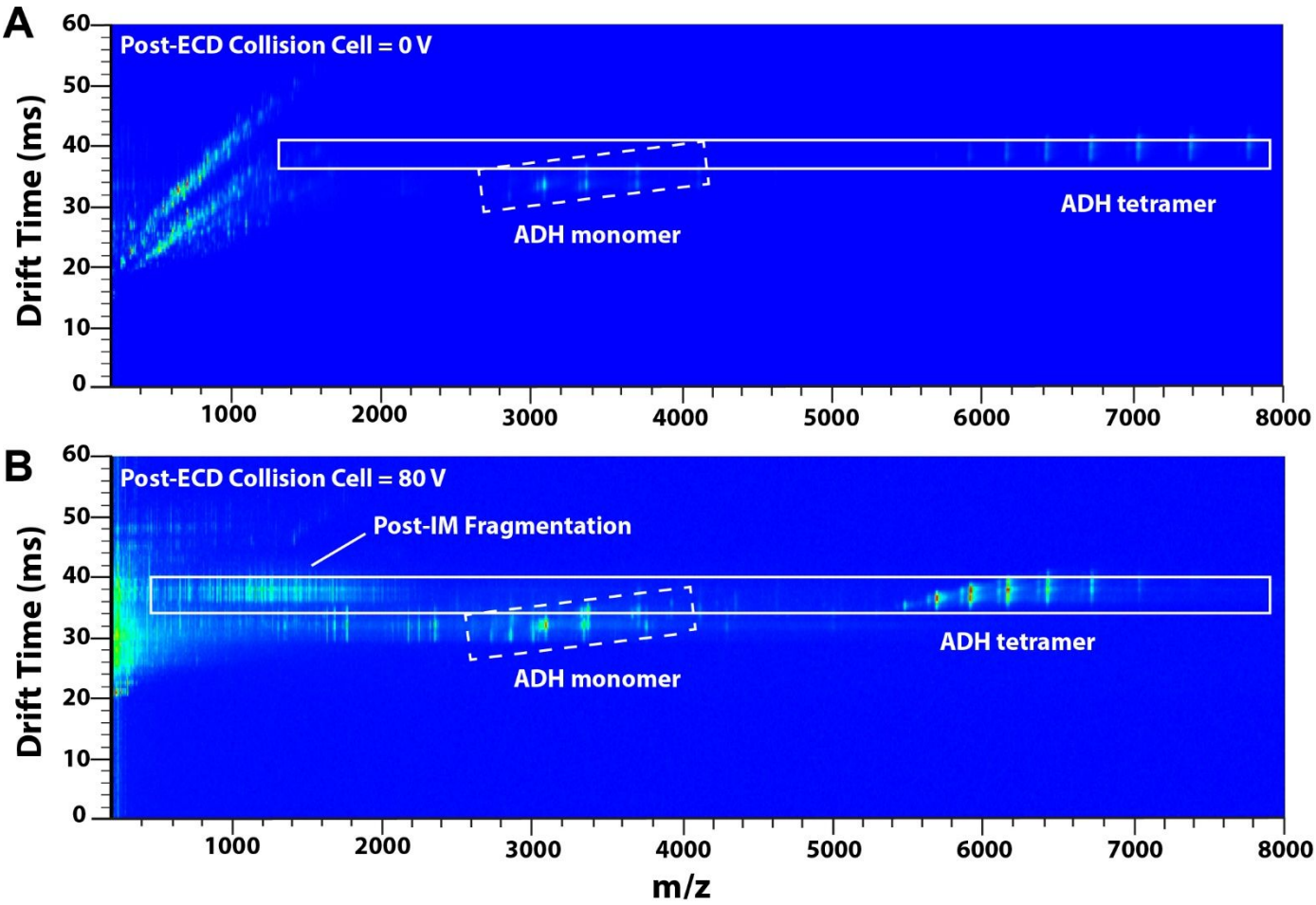

Figure S5: **80 V post-ECD activation is required to release ECnoD fragments**

(A) Alcohol Dehydrogenase tetramer at 100 V in-source collision voltage with ECD filament at 1.2 A. Scans were accumulated for an hour. No apparent ECD fragments visible **(B)** Alcohol Dehydrogenase at 100 V in-source collision voltage with ECD filament at 1.2 A and 80 V of activation in the post-ECD collision cell. Scans were accumulated for an hour. With some supplemental post-ECD activation, the ECD fragments are released from the precursor ion. ECD fragmentation occurs after IM, therefore the fragments are in the same drift time space as their precursor ion. Both fragments and precursor are enclosed by white boxes. The monomer is enclosed by a dashed white box. Buffer impurities are observed in the low m/z range due the absence of quad selection.

Figure S6

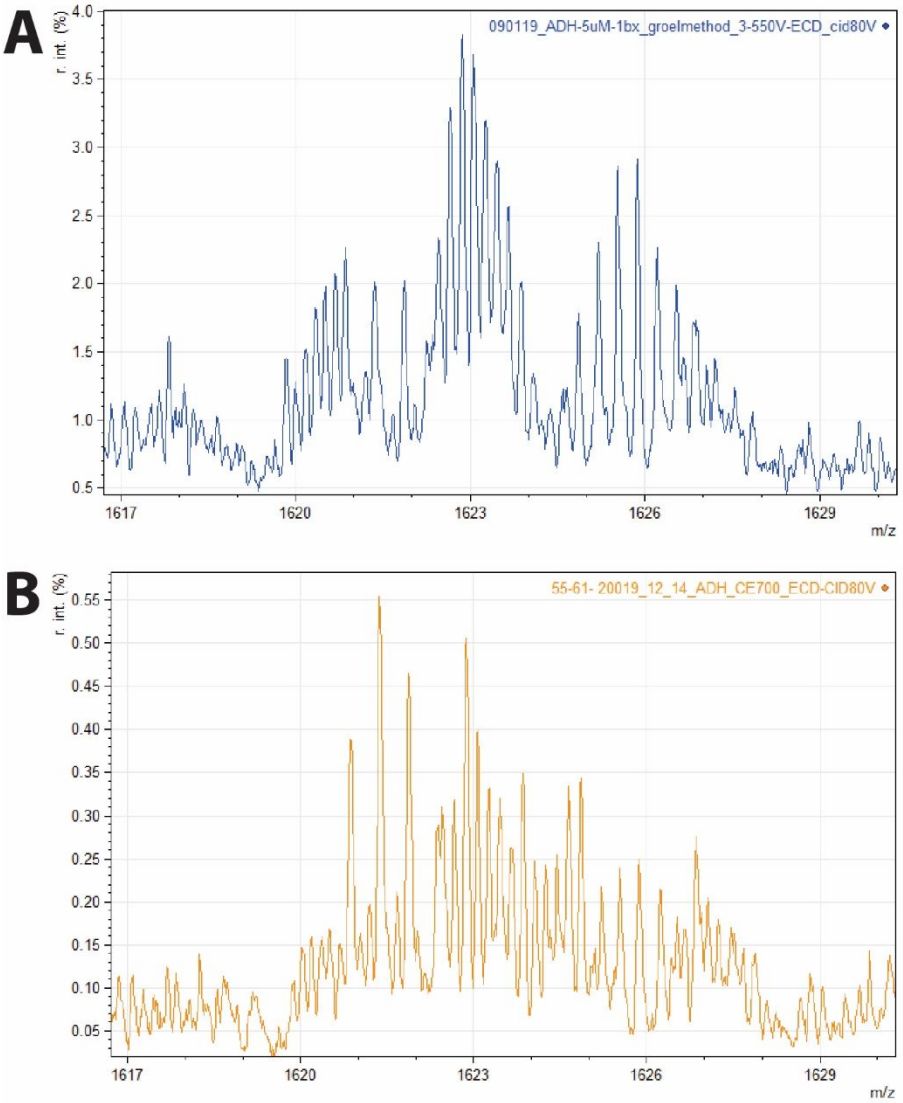

Figure S6: **Increased Spectral Complexity Upon Post-ECD CID of In-Source Activated ADH**

Although the ground state (in-source CID = 100 V) ADH tetramer ions require supplemental post-ECD activation to release ECD fragments, the activated ADH ions (in-source CID = 400 V) did not exhibit ECnoD. Addition of post-ECD collisional energy actually resulted in a reduction of fragments identified due to higher spectral complexity. **(A)** Alcohol Dehydrogenase tetramer at 400 V with ECD filament at 1.2 A. Scans were accumulated for an hour. **(B)** Alcohol Dehydrogenase at 400 V in-source activation with ECD filament at 1.2 A and 80V of activation in the post-ECD collision cell. The decline in spectral quality, resulted in lower quality peak picking, and thus fewer fragments were identified.

Figure S7

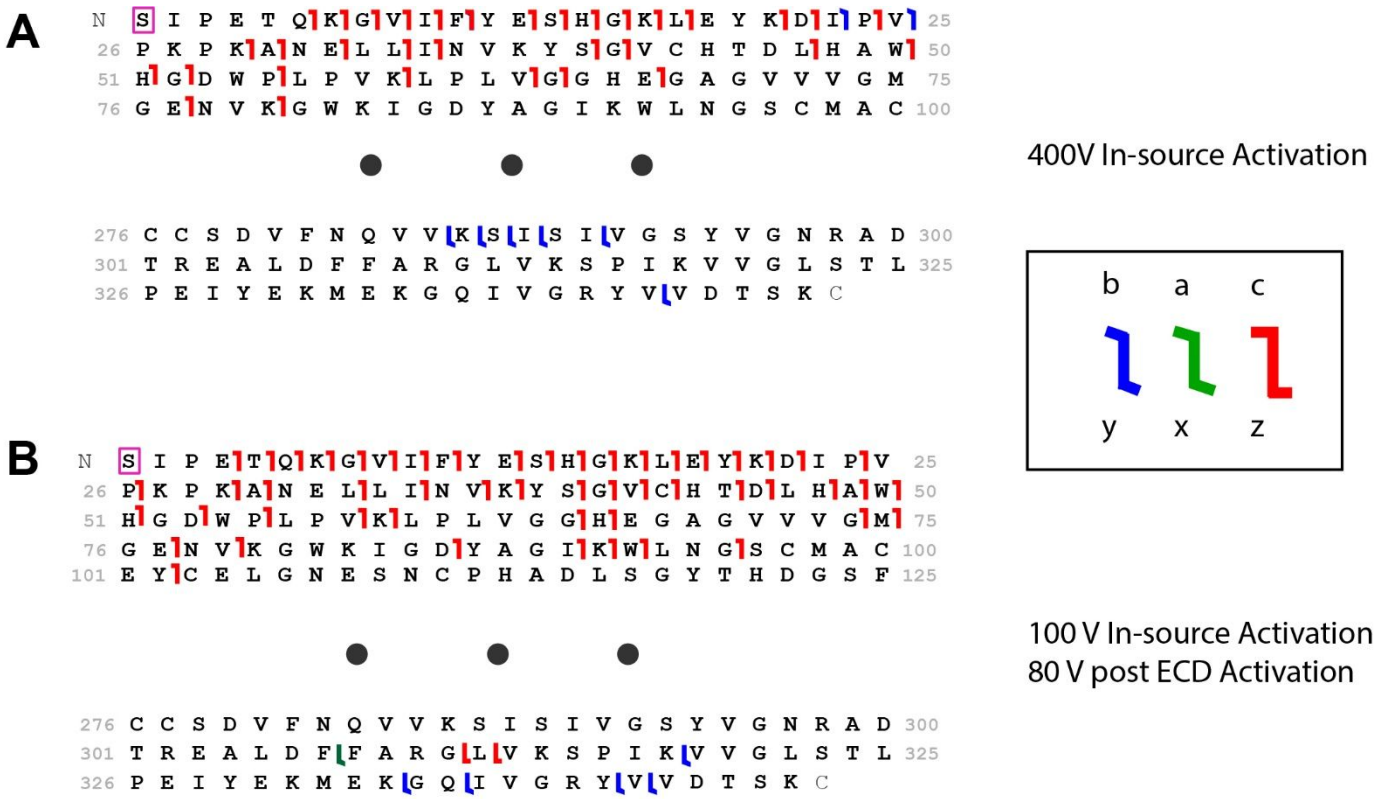

Figure S7: Sequence Coverage of ADH by Activated IM-ECD

ProSight Projections of ADH sequencing experiments. Sequence used for ADH (UniProt P00330) fragmentation analysis. Two substitutions were made to the UniProt sequence, V58T and I151V as confirmed by peptide mapping experiments by Zhou et al.[1]

SIPETQKGVIFYESHGKLEYKDIPVPKPKANELLINVKYSGVCHTDLHAWHGDWPLP**T**KLPLVGGHEGAGVVVGMGENVKGWKIGDYAGI
KWLNGSCMACEYCELGNESNCPHADLSGYTHDGSFQQYATADAVQAAHIPQGTDLAQVAP**V**LCAGITVYKALKSANLMAGHWVAISGA
AGGLGSLAVQYAKAMGYRVLGIDGGEGKEELFRSIGGEVFIDFTKEKDIVGAVLKATDGGAHGVINVSVSEAAIEASTRYVRANGTTVLVG
MPAGAKCCSDVFNQVVKSISIVGSYVGNRADTREALDFFARGLVKSPIKVVGLSTLPEIYEKMEKGQIVGRYVVDTSK

(A) ECD and CID fragment ions obtained at 400 V in-source activation. **(B)** ECD and CID fragment ions obtained at 100 V in-source activation with 80 V of supplemental activation after ECD, as described in **Figure S3**.

Figure S8

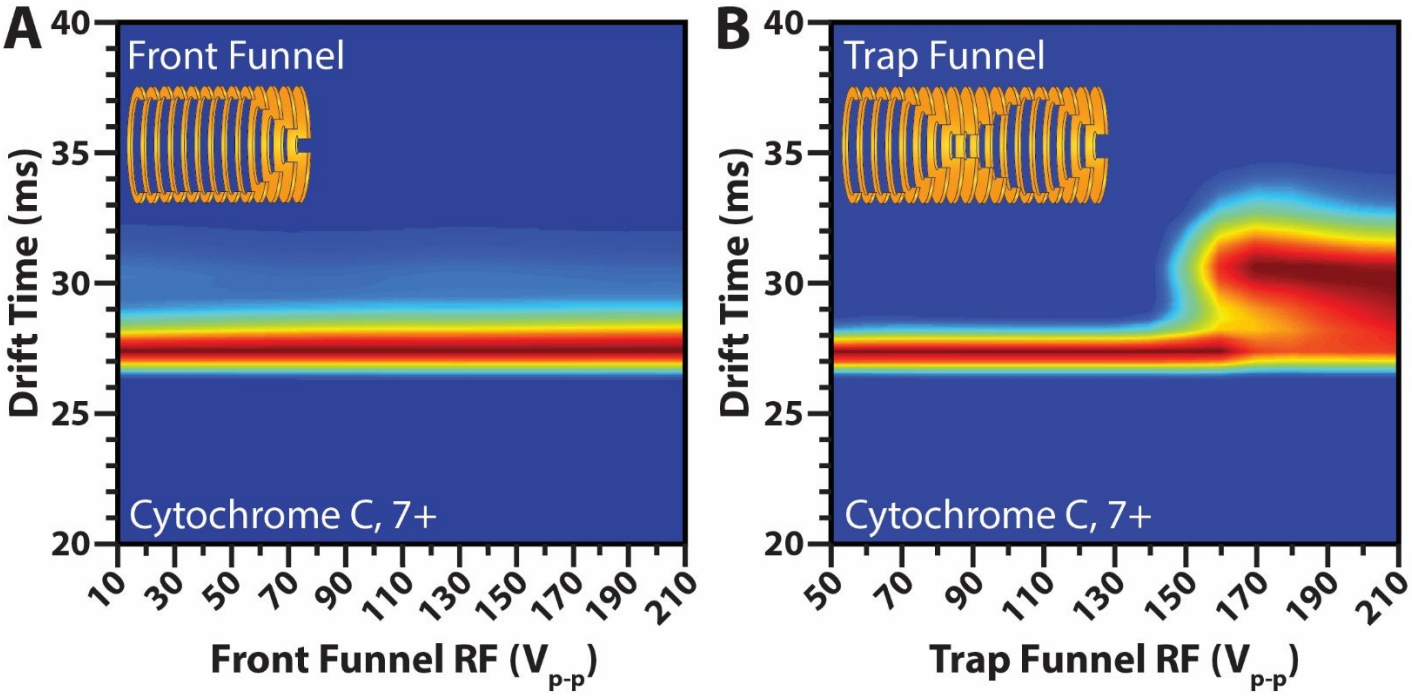

Figure S8: Evaluating the Activation of Cytochrome C 7+ by pre-IM Funnel Radio Frequency Confinement

Previous studies have demonstrated the capability of Radio Frequency (RF) confinement to activate ions. We used the 7+ ion of cytochrome C, a known fragile ion, to determine if the RF amplitudes in the high-pressure front funnel, or trap funnel were capable of unfolding native ions. The trap fill time was set to 10 ms, and trap release time was set to 1 ms. **(A)** Increasing the front funnel RF amplitude while maintaining trap funnel RF at 150 V had no effect on the ATD of Cytochrome C 7+. **(B)** The ATD of the 7+ ion was extended and, even unfolded once the trap funnel RF was increased beyond ~160 V_{p-p}, while maintaining a front funnel RF of 180V. Based on these findings, for all measurements reported, the front funnel RF was operated at 180 V_{p-p} to optimize ion transmission, while the trap funnel RF was operated at 150 V_{p-p} to minimize ion activation.

Table S1. $^{DT\text{-}SF}CCS_{N2}$ Measurements of GroEL Subcomplexes Table S1. $^{DT\text{-}SF}CCS_{N2}$

GroEL Subcomplex	MW	z	Avg. $^{DT\text{-}SF}CCS_{N2}$ (Å^2)	R.S.D.
GroEL Monomer	57,450	16	4098	3.10
		15	3975	2.88
		14	3884	1.91
		13	3794	0.54
GroEL Dimer	114,770	23	6391	1.28
		22	6288	0.93
		21	6149	0.49
		20	6042	2.39
GroEL Trimer	172,350	28	8648	0.95
		27	8449	0.40
		26	8318	0.22
		25	8187	0.84
GroEL Tetramer	229,930	32	10546	0.57
		31	10424	1.61
		30	10305	2.22
GroEL Pentamer	287,600	36	11580	0.94
		35	11492	0.98
		34	11490	0.77
GroEL Heptamer	402,340	46	14905	0.43
		45	14867	0.44
		44	14829	0.23
		43	14768	0.13
		42	14655	0.51
GroEL Tetradecamer	808400	71	21110	0.42
		70	21131	0.39
		69	21179	0.37
		68	21193	0.33
		67	21199	0.39
		66	21145	0.42
		65	21170	0.38
GroEL 28mer	1,608,660	102	36568	1.94
		101	36451	2.25
		100	36318	2.04
		99	36232	2.18
		98	36085	2.56

Table S2. IM-ECD Experiments and Sequence Coverage

Experiment Condition	# of Unique Fragments	Sequence Coverage (%)	Ion Type c	z	b	y	a	x
1. 400 V pre-IM CID + (No IM Separation)	23	7	19			4		
2. 400 V pre-IM CID + ECD (No IM Separation)	33	10	33					
3. 400 V pre-IM CID + 80 V post-IM CID	9	3			2	7		
4. 400 V pre-IM CID + post-IM ECD – IM Separated	43	13	33		2	8		
5. 400 V pre-IM CID + ECD + 80 V post-IM CID (IM Separated)	32	10	31			1		
6. 100 V pre-IM CID + ECD + 80 V post-IM CID (IM Separated)	64	20	52	2	5	4	1	
7. Combined Unique Fragments from Expts. 4 & 6	81	25	61	2	7	10	1	

Table S3. $^{DT}CCS_{N2}$ Measurements of Standard Proteins

ID	MW (Da)	n	z	$^{DT\text{-}SF}CCS_{N2}$ (Å²)	$^{DT\text{-}SF}CCS_{N2}$ R.S.D (%)	$^{DT\text{-}MF}CCS_{N2}$ (Å²)	$^{DT\text{-}MF}CCS_{N2}$ R.S.D (%)	Organism	Source
Insulin	5800	1	3	873	0.19	891	0.22	Human	Sigma I2643
Insulin	5800	1	4	917	0.17	921	0.11		
Insulin	11600	2	5	1392	0.15	1403	0.21		
Insulin	11600	2	6	1451	0.14	1472	0.20		
ubiquitin	8600	1	4	1113	0.50	1106	0.45	bovine eryth.	Sigma U6253
ubiquitin	8600	1	5	1145	0.41	1192	0.34		
ubiquitin	8600	1	6	1191	0.42	1145	0.26		
ubiquitin	8600	1	6	1345	0.64	1381	0.51		
ubiquitin	8600	1	6	1466	0.88	1444	1.04		
cytochrome C	12400	1	6	1446	0.28	1475	0.34	equine heart	Sigma C7752
cytochrome C	12400	1	7	1488	0.22	1502	0.20		
β-lactoglobulin	18400	1	7	1877	0.20	1917	0.10	bovine milk	Sigma L7880
β-lactoglobulin	18400	1	8	1933	0.11	1972	0.05		
β-lactoglobulin	36800	2	12	3162	0.19	3202	0.16		
β-lactoglobulin	36800	2	13	3275	0.38	3327	0.21		
serum albumin	66500	1	14	4402	0.42	4500	0.13	bovine	Sigma A7030
serum albumin	66500	1	15	4452	0.43	4519	0.77		
serum albumin	66500	1	16	4526	0.41	4575	0.07		
serum albumin	66500	1	17	4577	0.40	4573	0.11		
concanavalin A	102700	4	19	5864	0.64	-	-	*C. ensiformis*	Sigma C2010
concanavalin A	102700	4	20	5904	0.76	-	-		
concanavalin A	102700	4	21	5953	0.62	-	-		
concanavalin A	102700	4	22	5975	0.70	-	-		
ADH	147600	4	24	7490	0.40	7522	0.20	*S. cerevisiae*	Sigma A7011
ADH	147600	4	25	7534	0.29	7425	0.15		
ADH	147600	4	26	7571	0.46	7457	0.19		
ADH	147600	4	27	7585	0.66	7525	0.11		
GDH	337100	6	37	12742	0.38	-	-	bovine liver	Sigma G7882
GDH	337100	6	38	12812	0.50	-	-		
GDH	337100	6	39	12862	0.74	-	-		
GDH	337100	6	40	12902	0.79	-	-		
GDH	337100	6	41	12950	0.74	-	-		
GroEL	808400	14	65	21110	0.38	20866	0.25	*E. coli*	Sigma C7688
GroEL	808400	14	66	21170	0.42	21310	0.22		
GroEL	808400	14	67	21199	0.39	21129	0.13		
GroEL	808400	14	68	21193	0.33	21387	0.10		
GroEL	808400	14	69	21179	0.37	21251	0.20		
GroEL	808400	14	70	21131	0.39	21340	0.13		
GroEL	808400	14	71	21145	0.42	20379	0.27		

Table S4. Comparison of Single Field and Multifield $^{DT}CCS_{N2}$ Measurements

ID	MW	n	Z	Avg. $^{DT\text{-}SF}CCS_{N2}$ (Å²)	Avg. $^{DT\text{-}MF}CCS_{N2}$ (Å²)	% Difference SF vs. MF
Insulin	5800	1	3	873	891	-2.0
Insulin	5800	1	4	917	921	-0.4
Insulin	11600	2	5	1392	1403	-0.8
Insulin	11600	2	6	1451	1472	-1.4
ubiquitin	8600	1	4	1113	1106	0.6
ubiquitin	8600	1	5	1145	1192	-3.9
ubiquitin	8600	1	6	1191	1145	4.0
ubiquitin	8600	1	6	1345	1381	-2.6
ubiquitin	8600	1	6	1466	1444	1.5
cytochrome C	12400	1	6	1446	1475	-2.0
cytochrome C	12400	1	7	1488	1502	-0.9
β-lactoglobulin	18400	1	7	1877	1917	-2.1
β-lactoglobulin	18400	1	8	1933	1972	-2.0
β-lactoglobulin	36800	2	12	3162	3202	-1.2
β-lactoglobulin	36800	2	13	3275	3327	-1.6
serum albumin	66500	1	14	4402	4500	-2.2
serum albumin	66500	1	15	4452	4519	-1.5
serum albumin	66500	1	16	4526	4575	-1.1
serum albumin	66500	1	17	4577	4573	0.1
ADH	147600	4	24	7490	7522	-0.4
ADH	147600	4	25	7534	7425	1.5
ADH	147600	4	26	7571	7457	1.5
ADH	147600	4	27	7585	7525	0.8
GroEL	808400	14	65	21110	20866	1.2
GroEL	808400	14	66	21170	21310	-0.7
GroEL	808400	14	67	21199	21129	0.3
GroEL	808400	14	68	21193	21387	-0.9
GroEL	808400	14	69	21179	21251	-0.3
GroEL	808400	14	70	21131	21340	-1.0
GroEL	808400	14	71	21145	20379	3.8

Table S5. Comparison of $^{DT}CCS_{N2}$, Modified DTIM-QTOF vs. Modified Q-TWIM-TOF[2]

ID	n	z	DTIM-QTOF $^{DT\text{-}SF}CCS_{N2}$ (Å²)	Mod. TWIM $^{DT\text{-}MF}CCS_{N2}$ (Å²)[2]	% Difference DTIM vs. Mod. TWIM
cytochrome C	1	6	1446	1490	-3.0
cytochrome C	1	7	1488	1590	-6.4
β-lactoglobulin	1	7	1877	1950	-3.7
β-lactoglobulin	1	8	1933	2030	-4.8
β-lactoglobulin	2	12	3162	3310	-4.5
β-lactoglobulin	2	13	3275	3430	-4.5
serum albumin	1	14	4402	4490	-2.0
serum albumin	1	15	4452	4490	-0.8
serum albumin	1	16	4526	4470	1.3
serum albumin	1	17	4577	4490	1.9
concanavalin A	4	19	5864	6060	-3.2
concanavalin A	4	20	5904	6080	-2.9
concanavalin A	4	21	5953	6090	-2.3
concanavalin A	4	22	5975	6050	-1.2
GDH	6	37	12742	13400	-4.9
GDH	6	38	12812	13400	-4.4
GDH	6	39	12862	13400	-4.0
GDH	6	40	12902	13400	-3.7
GDH	6	41	12950	13500	-4.1
GroEL	14	65	21110	21800	-3.2
GroEL	14	66	21170	22000	-3.8
GroEL	14	67	21199	22000	-3.6
GroEL	14	68	21193	21900	-3.2
GroEL	14	69	21179	21900	-3.3
GroEL	14	70	21131	21800	-3.1
GroEL	14	71	21145	21900	-3.4

Table S6. Interlaboratory Comparison of Collision Cross Section Measurements

ID	z	Gadkari-SF		Gadkari-MF		Pukala/Beck-MF[3]		Barran-MF[4]		McLean-MF[5]		Interlaboratory Average	
		Avg. RSD	0.53 ± 0.18	Avg. RSD	0.32 ± 0.26	Avg. RSD	1.53 ± 0.45	Avg. RSD	0.97 ± 0.58	Avg. RSD	1.31 ± 0.53	Avg. RSD	0.82 ± 0.73
		CCS (Å²)	R.S.D.	CCS (Å²)	R.S.D.	CCS (Å²)	R.S.D.	CCS (Å²)	R.S.D.	CCS (Å²)	R.S.D.	CCS (Å²)	R.S.D.
Ubq	4	-	-	-	-	967	1.6	-	-	949	2.20	**958**	**0.94**
Ubq	4	1113	0.50	1106	0.45	1116	1.1	-	-	1116	1.40	**1113**	**0.42**
Ubq	5	-	-	-	-	-	-	-	-	1011	1.70	-	-
Ubq	5	1145	0.41	1192	0.34	1139	1.1	-	-	1221	1.90	**1184**	**2.87**
Ubq	6	1191	0.42	1145	0.26	1196	0.9	-	-	1222	1.20	**1188**	**2.69**
Ubq	6	1345	0.64	1381	0.51	-	-	-	-	1474	1.20	-	-
Ubq	6	1466	0.88	1444	1.04	-	-	-	-	1628	0.80	-	-
CytC	6	-	-	-	-	1330	1.3	-	-	1360	0.96	**1345**	**1.12**
CytC	6	1446	0.28	1475	0.34	1449	1.8	1456	0.47	1477	0.41	**1464**	**0.82**
CytC	7	1488	0.22	1502	0.20	1508	0.9	1481	1.23	-	-	**1497**	**0.77**
CytC	7	-	-	-	-	-	-	1450	1.23	-	-	-	-
SA	14	4402	0.42	4500	0.13	4467*	2.2	4349	1.7	-	-	**4425**	**1.71**
SA	15	4452	0.43	4519	0.77	4404*	1.5	4392	2.18	-	-	**4456**	**1.43**
SA	16	4526	0.41	4575	0.07	4521*	1.9	4445	1.53	-	-	**4510**	**1.44**
SA	17	4577	0.40	4573	0.11	4576*	1.8	4506	1.77	-	-	**4540**	**0.74**
ConA	19	5864	0.64	-	-	-	-	5905	0.54	-	-	**5885≠**	**0.35**
ConA	20	5903	0.76	-	-	-	-	5913	0.09	-	-	**5908≠**	**0.08**
ConA	21	5952	0.62	-	-	-	-	5937	0.42	-	-	**5945≠**	**0.13**
ConA	22	5975	0.70	-	-	-	-	5890	0.58	-	-	**5933≠**	**0.72**
ADH	24	7490	0.40	7522	0.20	-	-	7427	0.71	-	-	**7475**	**0.64**
ADH	25	7534	0.29	7425	0.15	-	-	7429	0.94	-	-	**7427**	**0.03**
ADH	26	7571	0.46	7457	0.19	-	-	7424	0.49	-	-	**7441**	**0.22**
ADH	27	7585	0.66	7525	0.11	-	-	7470	0.68	-	-	**7498**	**0.37**
GDH	37	12742	0.38	-	-	12614	1.8	-	-	-	-	**12678≠**	**0.51**
GDH	38	12812	0.50	-	-	12781	1.3	-	-	-	-	**12797≠**	**0.12**
GHD	39	12862	0.74	-	-	12673	2	-	-	-	-	**12767≠**	**0.74**
GHD	40	12902	0.79	-	-	12745	2.3	-	-	-	-	**12824≠**	**0.61**
GDH	41	12950	0.74	-	-	12865	1	-	-	-	-	**12907≠**	**0.33**

*HSA $^{DT}CCS_{N2}$ $^{\neq DT\text{-}SF}CCS_{N2}$ values were used for comparisons Interlaboratory comparisons from 2 laboratories Interlaboratory comparisons from 3 laboratories

References

(1) Zhou, M.; Liu, W.; Shaw, J. B. Charge Movement and Structural Changes in the Gas-Phase Unfolding of Multimeric Protein Complexes Captured by Native Top-Down Mass Spectrometry. *Anal. Chem.* **2020**, *92* (2), 1788–1795. https://doi.org/10.1021/acs.analchem.9b03469.

(2) Bush, M. F.; Hall, Z.; Giles, K.; Hoyes, J.; Robinson, C. V.; Ruotolo, B. T. Collision Cross Sections of Proteins and Their Complexes: A Calibration Framework and Database for Gas-Phase Structural Biology. *Anal. Chem.* **2010**, *82* (22), 9557–9565. https://doi.org/10.1021/ac1022953.

(3) Harrison, J. A.; Kelso, C.; Pukala, T. L.; Beck, J. L. Conditions for Analysis of Native Protein Structures Using Uniform Field Drift Tube Ion Mobility Mass Spectrometry and Characterization of Stable Calibrants for TWIM-MS. *J. Am. Soc. Mass Spectrom* **2019**, *30* (2), 256–267. https://doi.org/10.1007/s13361-018-2074-z.

(4) France, A. P.; Migas, L. G.; Sinclair, E.; Bellina, B.; Barran, P. E. Using Collision Cross Section Distributions to Assess the Distribution of Collision Cross Section Values. **2020**. https://doi.org/10.1021/acs.analchem.9b05130.

(5) May, J. C.; Jurneczko, E.; Stow, S. M.; Kratochvil, I.; Kalkhof, S.; McLean, J. A. Conformational Landscapes of Ubiquitin, Cytochrome c, and Myoglobin: Uniform Field Ion Mobility Measurements in Helium and Nitrogen Drift Gas. *Int. J. Mass Spectrom.* **2018**, *427*, 79–90. https://doi.org/10.1016/j.ijms.2017.09.014.